# Geopositioning from Airborne Three-Line Scanner Imagery Using Different Camera Orientation Models


***Gan Tianhong and Yan Li***

***Photogrammetry and Remote Sensing.***

***Wuhan, Hubei, China***



## Abstract

Three-line scanner CCD stereo surveying camera is now considered to be used not only in space borne vehicle but also airborne one. This sort of camera characterizes the imagery with the invalidation of conventional co linearity-based model and impropriety of satellite sensor model. This paper addresses the method of position and attitude determination without enough original exterior orientation data. Besides, tests report the geometric accuracy obtained with three sorts of camera orientation models and try to find a relatively effective & simplified one. Results show that the precision of polynomial Model is better than others with RMSE nearly one pixel.


## Introduction

Three-line scanner (TLS) CCD stereo surveying camera, which appeared in early 1980's and can get Fore-looking Nadir-Looking Aft-looking imagery at the same time[1], was first used in space borne vehicle with the successful launch of IKONOS- in 1999. Now, people are looking forward it's usage in airborne vehicle because of its efficiency and capacity of stereo surveying at the same track.

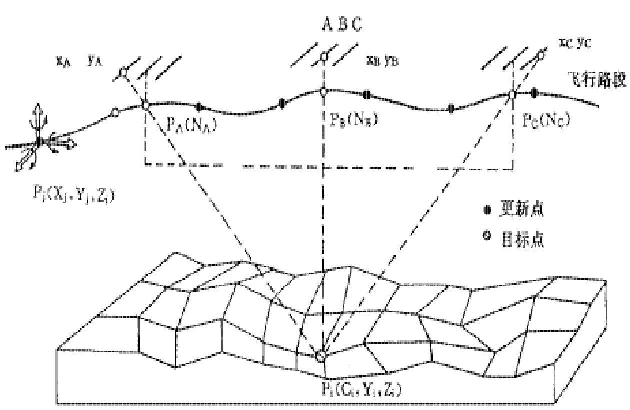


*Figure 1 photogrammetry model of TLS CCD stereo surveying camera*

High-resolution and seamless CCD image received from three angles can eliminate the disadvantage of obstruct caused by the terrain wave, especially high buildings in city[2], because at least from one angle, an image with good view can be received. In addition, TLS system is always collected together with GPS/INS systems, which can offer accurate Position and Orientation information of the camera, what result in a small quantity of ground control points.

Nowadays, some researchers around the world are engaging in the research of airborne three-line scanner imagery theory and processing method. Some methods such as DGR (Direct Georeferencing Model), PPM (Piecewise Polynomial Model), CSI (Cubic Spline Interpolation Model) are given by the Switzerland Union Technique and Photogrammetry Research Institution, as well as EFP (Equivalent frame photo) by Sian research institution of survey and mapping.

## Description of the method

At present, three-line CCD stereo mapping camera which is payload for three-dimensional surveying small satellite is being manufactured. However, airborne TLS scanner imagery is not available. In this paper, analog airborne TLS CCD imagery is used for a series of tests to evaluate the geometric accuracy with different camera orientation models and to find a relatively effective and simplified one.

### *A. Exterior orientation elements of the analog airborne TLS CCD image*

Produce the exterior orientation data as

$$p_i = a \cdot \cos(\frac{2\pi}{T} \cdot t) + b \cdot \sin(\frac{2\pi}{U} \cdot t) \qquad (1)$$

$$i = 1,2,\cdots 6$$

Where $p_i$ is one of the six exterior orientation elements ( $X_S, Y_S, Z_S, \varphi, \omega, \kappa$ ), t is time, and the other parameters of the equation1 see table1[3].

**Table1 parameters of the exterior orientation**

| $P_i$ | a | T | b | u |
|---|---|---|---|---|
| $X_s$ | 1.4 | 220 | 14 | 120 |
| $Y_s$ | 1.9 | 230 | 19 | 130 |
| $Z_s$ | 0.9 | 240 | 9 | 140 |
| $\varphi$ | 0.1 | 240 | 1 | 140 |
| $\omega$ | 0.01 | 320 | 0.5 | 220 |
| $\kappa$ | 0.1 | 220 | 1 | 120 |

Considering the observation error, a random error with mean square error 3m line elements and 0.00002 rad angle elements is added to the exterior orientation elements. Besides, base-height ratio of the image is 0.8, flying height is 8000 Km, and the photographic scale is 1:40000.

### B. Producing the analog airborne TLS CCD image

In this test, an image is divided to $11\times11=121$ grid points[4] equably, as well as the elevation to four coverage equably (24m 48m 72m 96m), which is among the range of height changes of the whole region. So $11\times11\times4$ grid points are obtained and for every coverage, there are the same elevation (Z) and 121 image points ($x, y$) respectively. Then, simulate the change of the exterior orientation to get the exterior orientation elements of every sample line. Besides, co- linearity-based model (see equation2.2) is used to calculate the horizontal coordinate ($X, Y$) of each grid point. After these steps, all coordinates of $11\times11\times4$ grid points can be acquired.

$$\begin{cases} X = \dfrac{F_1\cdot D_2 - F_2\cdot D_1}{F_1\cdot E_2 - F_2\cdot E_1} \\ Y = \dfrac{E_1\cdot D_2 - E_2\cdot D_1}{E_1\cdot F_2 - E_2\cdot F_1} \end{cases} \tag{2}$$

where

$E_1 = a_3\cdot x + a_1\cdot f$ $\qquad F_1 = b_3\cdot x + b_1\cdot f$

$E_2 = a_3\cdot y + a_2\cdot f$ $\qquad F_2 = b_3\cdot y + b_2\cdot f$

$$D_1 = (Z - Z_{Si})\cdot(-c_1 f - c_3 x) + (a_1 f + a_3 x)\cdot X_{Si} + (b_1 f + b_3 x)\cdot Y_{Si}$$

$$D_2 = (Z - Z_{Si})\cdot(-c_2 f - c_3 y) + (a_2 f + a_3 y)\cdot X_{Si} + (b_2 f + b_3 y)\cdot Y_{Si}$$

$a_1, a_2, a_3, b_1, b_2, b_3, c_1, c_2, c_3$ change with $\varphi_i, \omega_i, \kappa_i$

### C. Tests with different camera orientation models

Three sorts of camera orientation models are tested here.

◇ co linearity-based polynomial model

$$\begin{cases} x_i = -f\dfrac{a_1(X - X_{Si}) + b_1(Y - Y_{Si}) + c_1(Z - Z_{Si})}{a_3(X - X_{Si}) + b_3(Y - Y_{Si}) + c_3(Z - Z_{Si})} \\ y_i = 0 = -f\dfrac{a_2(X - X_{Si}) + b_2(Y - Y_{Si}) + c_2(Z - Z_{Si})}{a_3(X - X_{Si}) + b_3(Y - Y_{Si}) + c_3(Z - Z_{Si})} \end{cases} \tag{3}$$

Where

$$\begin{cases} X_{Si} = X_{S0} + \dot{X}_S\cdot y + \ddot{X}\cdot y^2 + \dddot{X}\cdot y^3 + \cdots \\ Y_{Si} = Y_{S0} + \dot{Y}_S\cdot y + \ddot{Y}\cdot y^2 + \dddot{Y}\cdot y^3 + \cdots \\ \ldots\ldots \\ \kappa_{Si} = \kappa_{S0} + \dot{\kappa}_S\cdot y + \ddot{\kappa}\cdot y^2 + \dddot{\kappa}\cdot y^3 + \cdots \end{cases}$$

◇ DLT(Direct Linear Transformation) model

$$\begin{cases} x = \dfrac{L_1\cdot X + L_2\cdot Y + L_3\cdot Z + L_4}{L_9\cdot X + L_{10}\cdot Y + L_{11}\cdot Z + 1} \\ y = L_5\cdot X + L_6\cdot Y + L_7\cdot Z + L_8 \end{cases} \tag{4}$$

◇ RFM(Rational Function Model )

$$\begin{cases} x = \dfrac{L_1\cdot X + L_2\cdot Y + L_3\cdot Z + L_4 + A\cdot \overline{X}}{L_9\cdot X + L_{10}\cdot Y + L_{11}\cdot Z + 1 + B\cdot \overline{X}} \\ y = \dfrac{L_5\cdot X + L_6\cdot Y + L_7\cdot Z + L_8}{L_{12}\cdot X + L_{13}\cdot Y + L_{14}\cdot Z + 1} \end{cases} \tag{5}$$

Where

$$A = (La_1, La_2, \cdots La_6)$$

$$B = (Lb_1, Lb_2, \cdots Lb_6)$$

$$\overline{X} = (XY, XZ, YZ, X^2, Y^2, Z^2)^{\mathrm{T}}$$

## Results and conclusion

**Table2 Results of co Linearity-based Polynomial Model (pixel)**

| No. | Dx(2nd power) | Dx(3rd power) | Dy(2nd power) | Dy(3rd power) |
|---|---|---|---|---|
| 1 | -3.047 | -1.096 | -2.376 | -0.368 |
| 2 | 1.694 | 0.407 | -1.396 | -0.410 |
| 3 | 2.098 | 1.152 | -1.403 | 0.580 |
| 4 | 0.000 | 0.000 | 0.000 | 0.000 |
| 5 | -1.558 | -1.697 | -1.885 | -0.883 |
| 6 | 0.551 | -0.722 | -1.309 | -0.784 |
| 7 | 0.584 | 1.026 | -1.506 | -1.120 |
| 8 | 1.002 | 1.417 | -1.799 | 0.069 |
| 9 | -0.936 | -1.271 | -1.380 | -0.505 |
| 10 | -0.331 | -0.634 | -1.246 | -1.383 |
| 11 | -0.001 | 0.000 | -0.000 | 0.000 |
| 12 | 0.001 | 0.000 | 0.001 | -0.000 |
| 13 | -0.767 | -0.241 | 1.676 | -1.973 |
| 14 | 0.150 | -0.649 | 1.291 | -0.610 |
| 15 | 0.027 | 1.178 | -1.613 | -0.717 |
| 16 | 0.454 | 1.295 | -1.692 | -0.334 |
| 17 | -0.264 | -0.839 | -1.344 | -0.861 |
| 18 | 0.031 | -0.585 | -1.282 | -1.025 |
| 19 | -2.643 | -1.262 | -2.595 | 0.274 |
| 20 | 0.352 | 0.766 | -1.730 | -0.887 |

**Table3 Results of co Linearity-based Polynomial Model (m)**

| No. | DX(2nd power) | DX(3rd power) | DY(2nd power) | DY(3rd power) |
|---|---|---|---|---|
| 1 | 4.9152 | 2.0514 | 6.4052 | 1.3459 |
| 2 | -3.1665 | -0.7458 | 3.0556 | 0.8824 |
| 3 | -3.9027 | -2.3660 | 3.1049 | -0.9592 |
| 4 | 0.0001 | 0.0000 | 0.0000 | 0.0000 |
| 5 | 1.9765 | 2.8087 | 4.4162 | 2.6028 |
| 6 | -0.9160 | 1.5897 | 2.7111 | 1.4491 |
| 7 | -1.6715 | -2.3908 | 2.7001 | 1.8016 |
| 8 | -2.8483 | -2.9498 | 3.2563 | -0.6958 |
| 9 | 1.8233 | 2.5100 | 2.7627 | 1.0259 |
| 10 | 0.6402 | 1.2409 | 2.4824 | 2.7602 |
| 11 | 0.0000 | 0.0000 | 0.0001 | 0.0000 |
| 12 | 0.0001 | 0.0000 | -0.0001 | 0.0000 |
| 13 | 2.9429 | -1.1190 | -2.7495 | 4.1676 |
| 14 | -0.7407 | 1.5160 | -2.4859 | 0.9929 |
| 15 | -0.6624 | -2.6022 | 3.1459 | 0.9726 |
| 16 | -1.5993 | -2.7848 | 3.2117 | 0.1739 |
| 17 | 0.4956 | 1.6517 | 2.6791 | 1.7285 |
| 18 | -0.0841 | 1.1446 | 2.5450 | 2.0463 |
| 19 | 4.0604 | 2.8725 | 6.7264 | 0.1634 |
| 20 | -0.4012 | -1.3656 | 3.4717 | 1.8788 |

**Table4 Results of DLT Model and RFM Model (pixel)**

| No. | Dx(DLT) | Dx(RFM) | Dy(DLT) | Dy(RFM) |
|---|---|---|---|---|
| 1 | 1.414 | -2.683 | -15.102 | -0.581 |
| 2 | -6.300 | 0.082 | -12.564 | -1.866 |

| | | | | |
|---|---|---|---|---|
| 3 | -5.232 | -0.869 | 28.094 | 7.407 |
| 4 | 5.858 | 0.597 | -12.244 | -0.912 |
| 5 | -15.080 | -1.989 | 27.051 | -0.339 |
| 6 | 11.922 | -2.471 | -45.607 | -6.249 |
| 7 | 2.594 | 6.671 | 21.750 | 2.404 |
| 8 | -4.779 | 1.778 | -25.971 | -6.993 |
| 9 | 4.451 | -2.931 | -32.297 | 0.626 |
| 10 | 9.472 | -0.078 | 30.740 | -1.084 |
| 11 | 10.899 | 6.255 | 5.722 | 5.226 |
| 12 | 6.730 | 0.124 | -7.527 | -5.856 |
| 13 | 5.834 | 0.901 | 2.134 | 3.858 |
| 14 | -23.063 | 2.941 | 5.876 | -0.671 |
| 15 | 12.103 | 5.354 | 13.407 | -0.883 |
| 16 | 5.753 | 0.330 | -17.107 | -2.017 |
| 17 | 0.059 | -0.582 | -13.899 | -0.678 |
| 18 | 2.656 | -0.889 | 12.272 | 0.458 |
| 19 | -18.027 | -8.921 | -22.970 | -7.244 |
| 20 | 17.507 | -7.358 | 37.045 | -0.626 |

In these tests, 25 ground control points and 20 check points are used equally. From the result, we can see that

- The precision of co Linearity-based Polynomial Model is better than others, because it is based on the physical sensor model and stricter theoretically. for 2nd power Polynomial, the Root Mean Square Error(RMSE) is: $m_x$ = 1.2 pixel, $m_y$ =1.5pixel; for 3rd power Polynomial, the RMSE is: $m_x$ = 0.9 pixel $m_y$ =0.8 pixel. 3rd power Polynomial is better than 2nd power Polynomial, but the advance is not very markedly.
- For DLT model, the RMSE is: $m_x$ = 10.3 pixel $m_y$ =22.4 pixel; and for RFM model, $m_x$ = 3.8 pixel $m_y$ =3.0 pixel. These two models are general sensor model which don't need position and orientation information of the camera.
- The expression of DLT is simple, and easy calculably, initialization is no longer necessary. Whereas, for co Linearity-based Polynomial Model, initialization is not only necessary, but also should be somewhat accurate, this will affect directly the number of calculation and the convergence.
- In RFM, 19 coefficients are used for sample direction(x) and only 7 coefficients for line direction(y), but the precisions are almost equal.
- There is instability for RFM , the precision do not improve with the number of control points or the power of Polynomial, more coefficients do not mean better precision.

## References


[1] Jin Guang, Payload of Stereo Mapping Small Satellite ---Three –Line CCD Stereo Mapping Camera, Remote Sensing Technology and Application, vol.14 No.3 1999

[2] Wang Renxiang, EFP Aerial Triangulation of Satellite Borne Three-Line Array CCD Image, Science of Surveying and Mapping, vol.26 No.4 2001

[3] Wang Renxiang, a Simulation Study on Bundle Adjustment from Space Using Three CCD Linear Scanner Imagery. Journal of Wuhan Technical University of Surveying and Mapping,, vol.23 No.4 1998

[4] Gong Danchao. Models and Algorithms on processing of High-Resolution Satellite Remote Sensing Stereo Images. Doctor Dissertation


## Author Biography

*Tianhong Gan a Ph.D. candidate in School of Geodesy and Geomatics Wuhan University, have worked in Jiangxi bureau of surveying and mapping for many years. she gained a master's degree in photogrammetry and remote sensing in 2003, now engage in the research of airborne three-line scanner(TLS) imagery theory and processing method, which is a project supported by the committee of national nature science fund.*